Modeling Second-Order Nonlinear Effects in Optical Waveguides Using a Parallel-Processing Beam Propagation Method

Husain M. Masoudi and John M. Arnold

Abstract— **In this work, we present a simple efficient numerical solution for the three-dimensional coupled wave equations containing a second-order nonlinearity, using an explicit finite-difference beam propagation method (EFD-BPM). The linear EFD-BPM is known to be very efficient and to gain large speed up when implemented on parallel computers. The new nonlinear version of the EFD-BPM has the same features of the linear counterpart in using two separate computational windows, one for the fundamental field and the other for the second-harmonic field. We demonstrate the implementation and discuss the application of this method to a nonlinear rib waveguide using the quasi-phase-matching technique.**

I. Introduction

RECENT experimental advances in the nonlinear effects of optical waveguides show that there is a need to model such devices accurately and efficiently ([1]–[4], and references therein). Waveguides that contain second-order nonlinear susceptibility (and nonlinear effects in general) are very difficult to model using analytically based techniques like coupled mode theory, and even more difficult when the devices contain multiple waveguides in which they have geometrical and/or material change in all three directions. Other methods, based on numerical analysis, are much better suited to such devices. The beam propagation method (BPM) is a well-known numerical method used, in different forms, to study many optical waveguides (a recent review of the BPM can be found in [5]). The method is attractive because it is suitable to study a wide range of different waveguides in addition to its simplicity and flexibility as a general propagational technique. For second-harmonic optical devices, the BPM has been used to simulate two-dimensional (2-D) [6], [7] and three-dimensional (3-D) [8] (fibers, with the assumption that the source field is undepleted) devices in both FFT and finite-difference (FD) forms.

In earlier work [9], [10], we have shown that implementations of the explicit FD method (EFD-BPM) and the real space method (RS-BPM) on parallel machines will speed up their execution times tremendously because of their nature as explicit methods which reduces communication between the parallel processors. On the other hand, other BPM methods do not possess this feature and consequently are not highly parallel and will not gain as much in speed up in the parallel environment [9], [10], [13]. Also it has been demonstrated that the parallel EFD-BPM is several times faster, per propagational step, than the parallel RS-BPM [9], [10], [13].

In this paper, we apply the parallel EFD-BPM to study 3-D waveguides in the presence of a second-order nonlinearity $\chi^{(2)}$ where the source field is allowed to deplete. We will refer to this method as the parallel second-harmonic generation EFD-BPM (or in short SHG-EFD-BPM). Early results of this method have been reported in a short communication [12], while in this paper, we show the full analysis without concentrating on the issue of parallel implementation. In Sections II and III, we discuss the derivation and the implementation of the numerical nonlinear coupled wave equations both in 3-D (SHG-EFD-BPM) and in 1-D, which is commonly used in the literature to validate experimental results and to study possible concepts for optical devices [1], [3], [4]. Then, in Section IV, we analyze, using the parallel SHG-EFD-BPM, a semiconductor rib waveguide containing a second-order nonlinearity with quasi-phase matching (QPM) [14], [15] to model the relative phase between the fundamental and the second-harmonic fields. Also in the same section, we compare and discuss the parallel SHG-EFD-BPM results with the solution of the reduced 1-D coupled wave equations [16].

II. Numerical Methods

The wave equation for the propagation of an electric field E of a given polarization in a material with a refractive index n can be written as

$$\nabla^2 E = \mu_0 \epsilon_0 n^2 \frac{\partial^2 E}{\partial t^2} + \mu_0 \epsilon_0 \frac{\partial^2 P}{\partial t^2}, \tag{1}$$

where ∇^2 is the Laplacian operator, the speed of light in vacuum is $c = 1/\sqrt{\mu_0 \epsilon_0}$ and P is the nonlinear polarization in the material that can be approximated, for CW operation, as $P = \chi^{(2)} EE$ with $\chi^{(2)}$ being the second-order nonlinear susceptibility of the material.

Manuscript received January 20, 1995; revised July 19, 1995. This work was supported in part by the Science and Engineering Council under Research Grant GR/H82471.

H. M. Masoudi is with the Department of Electrical Engineering, King Fahd University of Petroleum and Minerals, Dhahran 31261, Saudi Arabia.

J. M. Arnold is with the University of Glasgow, Glasgow, Scotland, UK.

IEEE Log Number 9415440.

Let us now consider the propagation of two fields at two different frequencies, one at ω (the fundamental field) and the other at 2ω (the second-harmonic field), while extracting a common reference phase in the direction of propagation z. Then the fields can be written as

$$E^{\omega}(x, y, z, t) = \frac{1}{2}[\Phi^{\omega}(x, y, z)e^{j(\omega t - k_o n_o z)} + \text{c.c.}] \quad (2a)$$

$$E^{2\omega}(x, y, z, t) = \frac{1}{2}[\Phi^{2\omega}(x, y, z)e^{2j(\omega t - k_o n_o z)} + \text{c.c.}], \quad (2b)$$

where n_o is a reference refractive index, k_o is the free-space wave at the fundamental frequency defined as $k_o = \frac{2\pi}{\lambda_f}$ and c.c. is the complex conjugate. Inserting (2) in (1), and neglecting terms containing second derivatives with respect to z, we arrive at the coupled parabolic wave equations in three dimensions for both the fundamental and the second-harmonic waves

$$2jk_o n_o \frac{\partial \phi^f}{\partial z} = \frac{\partial^2 \phi^f}{\partial x^2} + \frac{\partial^2 \phi^f}{\partial y^2} + k_o^2(n_f^2 - n_o^2)\phi^f + k_o^2 \chi^{(2)} \phi^s \phi^{f*} \quad (3a)$$

$$4jk_o n_o \frac{\partial \phi^s}{\partial z} = \frac{\partial^2 \phi^s}{\partial x^2} + \frac{\partial^2 \phi^s}{\partial y^2} + 4k_o^2(n_s^2 - n_o^2)\phi^s + 2k_o^2 \chi^{(2)} \phi^f \phi^f, \quad (3b)$$

where ϕ^f and ϕ^s are the parabolic fields of the fundamental and the second-harmonic respectively, which are paraxial approximations to the Φ's (the Helmholtz fields) in (2). Here, we assume that the fields are linearly polarized and that the vector nature of the fields can be ignored. This is a good first approximation for paraxial problems of the type considered here for which the BPM is appropriate. Throughout this paper, subscripts or superscripts for both f and s are related to the fundamental wave and the second-harmonic wave, respectively. In the derivation of (3), we have assumed that the second-order nonlinearity is homogeneous and is defined through $\chi^{(2)} = \chi^{(2)}(2\omega; \omega, \omega) = \chi^{(2)}(\omega; 2\omega, -\omega)/2$ [1], [3] and the source field is allowed to deplete during propagation. We use central finite-difference approximations for the partial derivatives acting on a field F in (3)

$$\left.\begin{aligned} \frac{\partial^2 F(\rho)}{\partial \rho^2} &= \frac{F(\rho+\Delta\rho) - 2F(\rho) + F(\rho-\Delta\rho)}{\Delta\rho^2}, \quad (\rho = x, y) \\ \frac{\partial F(z)}{\partial z} &= \frac{F(z+\Delta z) - F(z-\Delta z)}{2\Delta z} \end{aligned}\right\}, \quad (4)$$

where $\Delta\rho$ and Δz are the transverse mesh size and the stepping of the field in the direction of propagation z respectively. Then (3) can be discretized with second-order accuracy with respect to z as [9]–[13]

$$\phi_{i,m}^f(z + \Delta z) = \phi_{i,m}^f(z - \Delta z) + d_x[\phi_{i+1,m}^f(z) + \phi_{i-1,m}^f(z)] + d_y[\phi_{i,m+1}^f(z) + \phi_{i,m-1}^f(z)] + b_f \phi_{i,m}^f(z) + \alpha \phi_{i,m}^s(z) \phi_{i,m}^{f*}(z) \quad (5a)$$

$$\phi_{i,m}^s(z + \Delta z) = \phi_{i,m}^s(z - \Delta z) + \frac{d_x}{2}[\phi_{i+1,m}^s(z) + \phi_{i-1,m}^s(z)] + \frac{d_y}{2}[\phi_{i,m+1}^s(z) + \phi_{i,m-1}^s(z)] + b_s \phi_{i,m}^s(z) + \alpha \phi_{i,m}^f(z) \phi_{i,m}^f(z), \quad (5b)$$

where

$$d_\rho = -j\frac{\Delta z}{n_o k_o \Delta\rho^2}, \quad (\rho = x, y)$$

$$b_f = -j\frac{\Delta z}{n_o k_o}\left[-\frac{2}{\Delta x^2} - \frac{2}{\Delta y^2} + k_o^2(n_f^2 - n_o^2)\right]$$

$$b_s = -j\frac{\Delta z}{2n_o k_o}\left[-\frac{2}{\Delta x^2} - \frac{2}{\Delta y^2} + 4k_o^2(n_s^2 - n_o^2)\right]$$

$$\alpha = -j\frac{\Delta z k_o \chi^{(2)}}{n_o},$$

where i and m represent the discretization of the transverse coordinates x and y.

Let us also write the usual approximate 1-D coupled wave equations for the nonlinear wave equation; later in this work, we use the solution of the 1-D equations to compare with the results of the SHG-EFD-BPM. The derivation of the 1-D approximation is the same as our 3-D approach without x and y variations. If we project the fields onto the 3-D eigen functions (the mode distributions) and write the 3-D fields in (3) as

$$\left.\begin{aligned} \phi^f &= \frac{E^f \Psi^f}{\sqrt{R_1 R_2}} \\ \phi^s &= \frac{E^s \Psi^s}{R_1} \end{aligned}\right\}, \quad (6)$$

where

$$R_1 = \frac{S_o}{S_1}, \qquad R_2 = \frac{S_o}{S_2}$$

$$S_1 = \iint_A (\Psi^f)^2 \, dA, \qquad S_2 = \iint_A (\Psi^s)^2 \, dA$$

$$S_o = \iint_A (\Psi^f)^2 \Psi^s \, dA,$$

the E's are dependent only on z, Ψ's are the 3-D z-independent linear mode fields and A is the cross-sectional area. Inserting (6) in (3), the 1-D nonlinear coupled wave equations can be written as [1], [3]

$$\frac{dE^f}{dz} = -j\frac{k_o \chi^{(2)}}{2n_f^{\text{eff}}} E^s E^{f*} e^{-j\Delta k' z} \quad (7a)$$

$$\frac{dE^s}{dz} = -j\frac{k_o \chi^{(2)}}{2n_s^{\text{eff}}} E^f E^f e^{j\Delta k' z}, \quad (7b)$$

where the wave vector mismatch is $\Delta k' = 2k_o(n_s^{\text{eff}} - n_f^{\text{eff}})$ (note that the extracted reference phase is not common for both fields). From the power relation ($P = \frac{nE^2}{2Z_o} A_{\text{eff}}$, Z_o is the free space impedance) we can also express the effective area of the 3-D fields as

$$A_{\text{eff}} = \frac{S_1^2 S_2}{S_o^2} \quad (8)$$

For perfect phase matching ($\Delta k' = 0$), (7) leads to the well-known solution for the normalized intensities of the fundamental and the second harmonic as

$$\left.\begin{aligned} \frac{I^f}{I_o} &= \text{sech}^2(\Gamma z) \\ \frac{I^s}{I_o} &= \tanh^2(\Gamma z) \end{aligned}\right\} \quad (9)$$

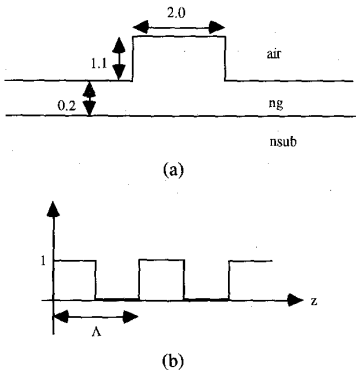

Fig. 1. (a) The rib waveguide used in the computations. (b) The rectangular periodic grating of the nonlinear medium.

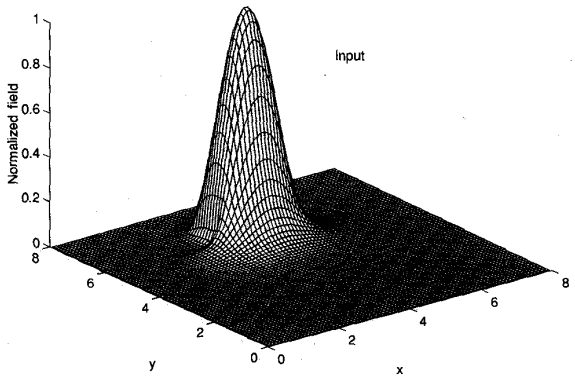

Fig. 2. The normalized field distribution of the first guided mode of the fundamental waveguide that has been used as an input for the analysis.

where

$$\Gamma = \frac{k_o \chi^{(2)} |E_o^f|}{2\sqrt{n_f^{\text{eff}} n_s^{\text{eff}}}}$$

and I_o and E_o^f are the initial intensity and field respectively of the fundamental at $z = 0$. For the nonphased-matched case (6) can be solved using Jacobian elliptic functions [3], [15] or numerically using the Runge–Kutta method [16]. We have used the fourth-order Runge–Kutta method to solve the 1-D coupled wave equation in (7) [16].

III. Implementations

We have implemented the SHG-EFD-BPM in (5) using two different parallel machines, a transputer array (MIMD machine) and a connection machine (SIMD machine). These implementations are similar to the linear ones in [9], [10] and also are described in [12], [13]. Two separate computational windows, one for the fundamental field and the other for the second-harmonic field, have been used while allowing them to share common data for the calculations of the coupled terms. It has been observed from testing the SHG-EFD-BPM that the method is stable for propagation steps Δz very close to the limiting values of the linear EFD-BPM in [9]–[11]. The reason for this is that the nonlinear term in (3) has very little effect on the stability of the method due to the small value of $\chi^{(2)}$, which is in the order of 10^{-12} m/V for practical devices [1], [3], [4]. As expected, the speeds of the parallel SHG-EFD-BPM implementations are more than twice as slow as the corresponding linear parallel EFD-BPM [12].

IV. Results and Discussions

Throughout this paper, we have used the rib waveguide in Fig. 1(a) to study a nonlinear semiconductor device with the following parameters (all dimensions are in μm) [3], [12]: $n_{\text{sub}} = 3.4$, $\lambda_f = 1.55$, $\lambda_s = 0.775$, $n_{gf} = 3.5$, $n_{gs} = 3.6$, $\chi^{(2)} = 300$ pm/V. The design of this structure shows that it is strongly guiding at both frequencies although it is a single-mode waveguide at the fundamental frequency and a multimode waveguide at the second-harmonic frequency. Using equal lengths of 8 μm for the x and y window sizes and $\Delta x = \Delta y = 0.1$, the computed first guided mode effective indices of both fields, using $\Delta z = 0.025$ and $n_o = n_{\text{sub}}$, are $n_f^{\text{eff}} = 3.45299169$ and $n_s^{\text{eff}} = 3.58591145$. The power spectral method in [17], [18] has been used to compute the linear mode effective indices and the field distributions of the structure from the BPM fields. Fig. 2 shows the normalized field distribution of the first guided mode of the fundamental waveguide. The computed effective area, using (8), of the 3-D fields is 1.92 μm^2. The parameters of this structure show that it is a nonphase matched waveguide in which quasi-phase matching (QPM) techniques could be used to alter the relative phase difference between the two fields [14], [15]. QPM is used for efficient optical SHG and other nonlinear optical processes [3], [14]. In practical terms, QPM is achieved by introducing structural periodic gratings, in the direction of propagation, of the nonlinear medium. The BPM mismatch wave vector, for QPM, is defined as $\Delta k = \beta_s^p - 2\beta_f^p - \frac{2\pi}{\Lambda}$, where β_f^p and β_s^p are the parabolic wave numbers of the fundamental and the second-harmonic fields respectively, and Λ is the grating period. The computed grating length, for $\Delta k = 0$ (between the first guided modes of both frequencies), of this waveguide is equal to 5.63269267 μm. In our simulation we have used a grating in which the second-order nonlinear coefficient $\chi^{(2)}$ has either its full value or is zero in alternate half-periods of the grating [see Fig. 1(b)]. This geometry might be realized in a semiconductor asymmetric quantum well by selective-area disordering, which periodically annihilates the $\chi^{(2)}$ coefficient produced by the quantum well breaking the symmetry of the bulk martial [19]. It is known that QPM reduces the effectiveness of the second-order nonlinear coefficient $\chi^{(2)}$ by a factor $2/\pi$ in the case of domain reversal and by a factor of $1/\pi$ in the case of domain disordering (where $\chi^{(2)}$ is periodically reduced to zero) [14], [15]. In the following computations, the first guided mode of the fundamental frequency (Fig. 2) has been launched as an input to the waveguide, and zero initial field is assumed for the second harmonic.

Fig. 3 shows the normalized intensities for both the fundamental and the second-harmonic modes along the propagation direction z for a grating length Λ =5.64 μm (ΔkL =

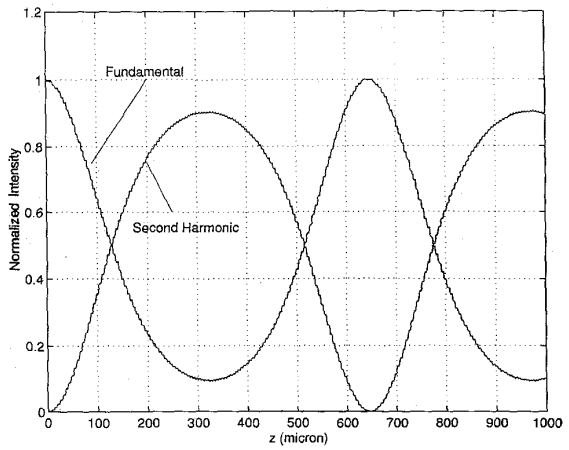

(a)

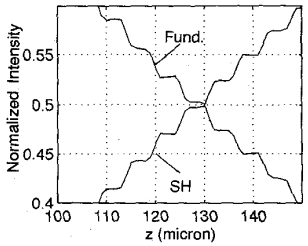

(b)

Fig. 3. (a) The normalized intensity for both of the fundamental and the second-harmonic fields versus the longitudinal distance $z(\mu m)$, using the parallel SHG-EFD-BPM with an input power = 125.6 W and a grating length $\Lambda = 5.64$ μm. (b) A portion from the top figure enlarged to show the ripple caused by the QPM.

1.445252). The computation of the normalized intensities of the modes has been carried out numerically by evaluating the square of the magnitude of the projected total BPM field onto the normalized mode and then normalizing with respect to the input intensity, which can be expressed as

$$I^{f,s}_{\text{norm}}(z) = \frac{\left| \iint_A \Psi^{f,s} \phi^{f,s}(z)\, dA \right|^2}{\iint_A |\Psi^{f,s}|^2\, dA \iint_A |\phi^f(0)|^2\, dA}, \qquad (10)$$

where f, s means the fundamental or the second harmonic. On the other hand, Fig. 4 shows the total normalized fields in the fundamental and second-harmonic windows at different propagational distances using the parameters of Fig. 3. From these two figures, the power exchange mechanism between the two modes is clearly shown, where the effect of the QPM has been demonstrated through the coupling and the ripple of the intensities shown in Fig. 3(b) with the grating periodicity. Fig. 4 shows that some power has coupled into radiation in the second-harmonic window. The computed radiation power is very small compared with the power carried by the first guided modes in both windows. Also it has been observed that there is very little coupling to the third-order mode of the second-harmonic where this can be explained from the overlap integral between the first-order mode at the fundamental frequency and the modes at the second-harmonic frequency, which is zero for the second-order mode and very small for the third-order mode [8] [see also S_o below (6)]. In addition, the grating length used, in this simulation, results in nonphase-matching for these modes.

In the following case, we compute, using the parallel SHG-EFD-BPM, the output depletion and the nonlinear phase change of the fundamental field after a distance of $L = 1$ mm for different grating lengths along the direction of propagation. By varying the grating length, the relative wave vector Δk changes while exciting predominately the first guided mode of the second-harmonic frequency. It has been assumed that the phase of the fundamental field is changing as $e^{-j(\beta_f^p z + \theta_{NL})}$ where θ_{NL} is the nonlinear phase shift of the fundamental field. In order to check the results of the parallel SHG-EFD-BPM, we have also run the approximate 1-D coupled wave equations [of (7)] using the fourth-order Runge–Kutta with the same parameters. There are two methods to simulate QPM technique using the solution of (7). The first method is to use exactly the same procedure of the 3-D BPM with actual structural periodic gratings for the second-order nonlinear coefficient $\chi^{(2)}$ along the z direction and the second method is to reduce the value of $\chi^{(2)}$ by the QPM factor $1/\pi$ or $2/\pi$ (without structural grating), while changing explicitly $\Delta k'$ to $\Delta k' = 2k_o(n_s^{\text{eff}} - n_f^{\text{eff}}) - \frac{2\pi}{\Lambda}$, in (7), to simulate the existence of second-order nonlinear gratings [1], [4]. We have tested both of these methods numerically using the fourth-order Runge–Kutta and we found excellent agreement between the two results. In the following simulation, we will use the second method to compare with the SHG-EFD-BPM results. Fig. 5 shows the depletion intensity and the nonlinear phase shift θ_{NL} of the fundamental as functions of ΔkL for both the parallel SHG-EFD-BPM and the approximate 1-D Runge–Kutta ($\Delta k'L = \Delta kL$) for different input powers. The figure shows close agreement between the two results. Also from the figure, we can see that the nonlinear phase shift can be positive or negative, depending on the grating period, and this phase shift is increasing when the input power is increased. This effect has been studied theoretically [3], [4], and has been observed experimentally in KTP [1]. In addition, Fig. 6 shows the dependence of the depletion and the nonlinear phase shift θ_{NL} of the fundamental on the input power using the parallel SHG-EFD-BPM and the approximate 1-D Runge–Kutta for several values of ΔkL ($\Delta k'L = \Delta kL$). From this figure, we notice that the two methods agree very closely at low power with some little deviation at high power. The propagation step size Δz used in these computations was 0.01 μm, although the SHG-EFD-BPM algorithm is stable for $\Delta z = 0.025$ μm, but in order to model the exact grating lengths mentioned before using a common step size, Δz had to be reduced. The total execution time for each run of the parallel SHG-EFD-BPM is around 10.3 min. on the connection machine (CM-200) using 16-k processors and around 76.3 min. using 64 processors of the transputer array [12], [13]. Since the transputer implementation runs at around 54.2% efficiency [10], [13], the serial execution time on one processor would be 2646.7 min., or 1.84 days.

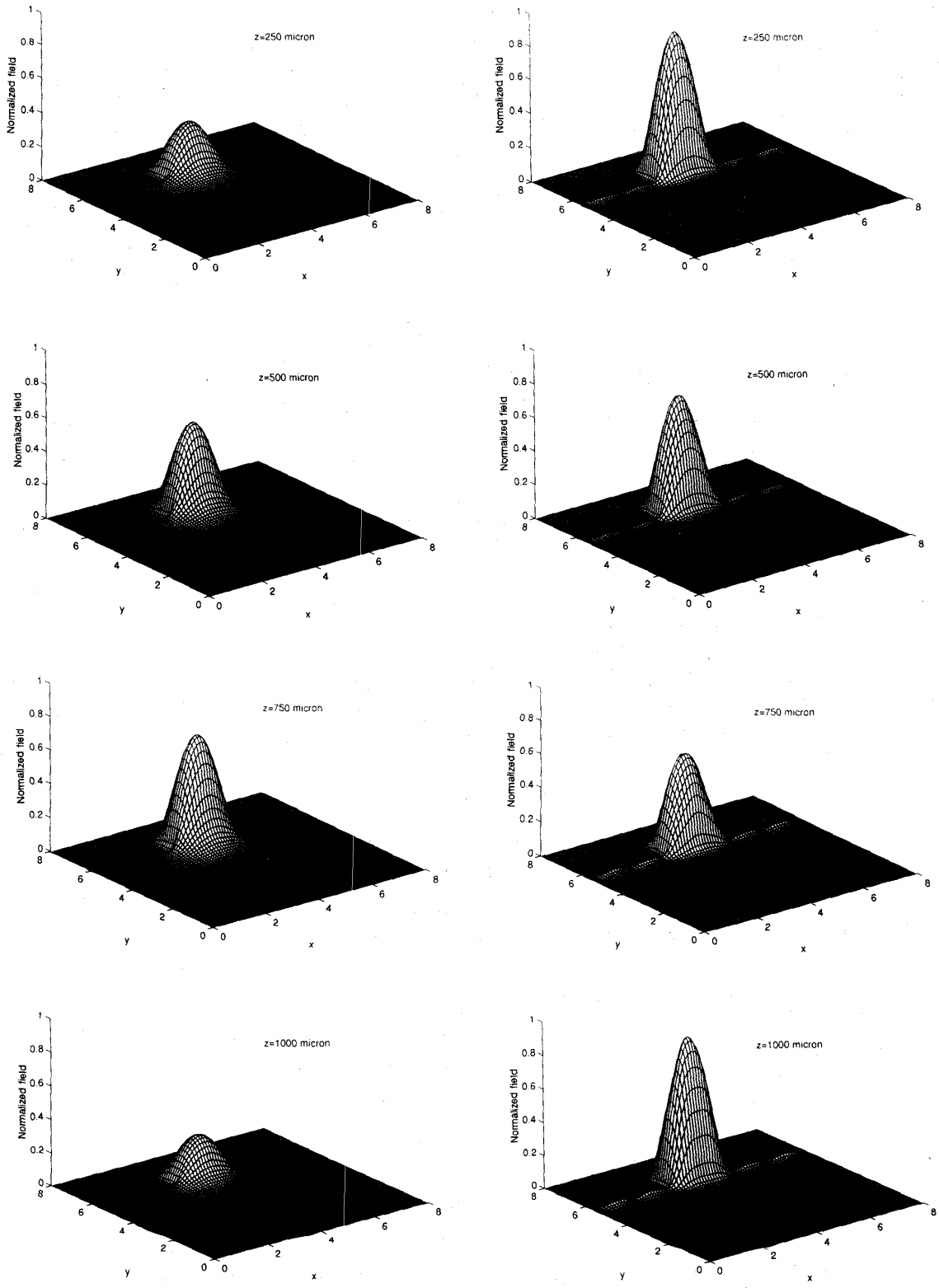

Fig. 4. The normalized total fields of the fundamental (left, top to bottom) and the second harmonic (right, top to bottom) at several propagational distances using the parallel SHG-EFD-BPM. All field points are normalized to 21.3×10^7 (see Fig. 3 for other details).

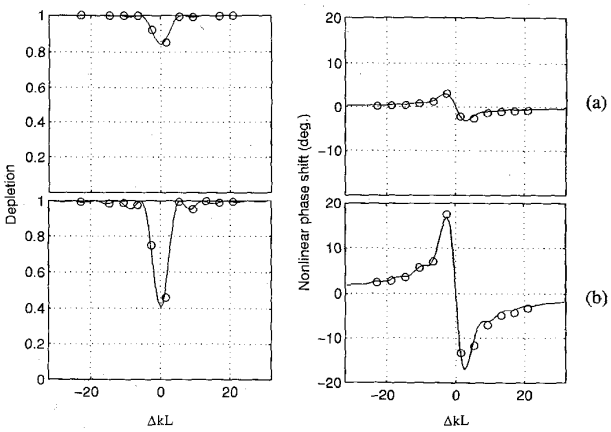

Fig. 5. The depletion intensity (left) and the nonlinear phase shift θ_{NL} (right) of the fundamental as functions of ΔkL ($\Delta k'L = \Delta kL$) using the parallel SHG-EFD-BPM (circles) and the 1-D Runge–Kutta (solid line) for (a) input power = 0.51 W and (b) input power = 3.02 W.

V. Conclusion

A numerical method to model three-dimensional optical waveguides containing a second-order nonlinearity has been presented. The new nonlinear method, which is an extension to the linear parallel EFD-BPM, is also highly parallel. We have implemented the method to model a semiconductor rib waveguide in the presence of the second-order nonlinearity $\chi^{(2)}$ where the source field is allowed to deplete, using two different supercomputers. The quasi-phase matching (QPM) technique has been realistically incorporated in the analysis of the waveguide in order to change the relative phase mismatch between the two fields. We have also implemented the approximate 1-D nonlinear coupled wave equations numerically using the Runge–Kutta method to validate some of the results of the nonlinear EFD-BPM. Excellent agreement between the two methods has been observed. Finally, it has been concluded that the new parallel algorithm is simple, efficient and very useful for modeling large complicated nonlinear optical devices.

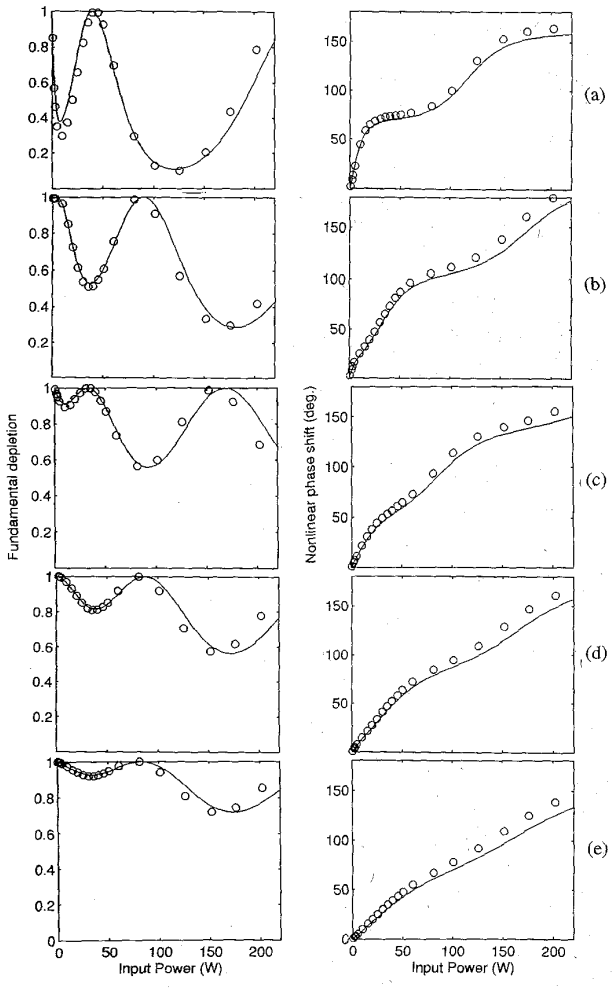

Fig. 6. The depletion intensity (left) and the nonlinear phase shift $|\theta_{NL}|$ (right) of the fundamental as functions of input power using the parallel SHG-EFD-BPM (circles) and the 1-D Runge–Kutta (solid line) for different values of ΔKL ($\Delta k'L = \Delta kL$). (a) $\Lambda = 5.64\ \mu$m ($\Delta kL = 1.44525$), (b) $\Lambda = 5.66\ \mu$m ($\Delta kL = 5.38179$), (c) $\Lambda = 5.68\ \mu$m ($\Delta kL = 9.29060$), (d) $\Lambda = 5.70\ \mu$m ($\Delta kL = 13.17199$), and (e) $\Lambda = 5.74\ \mu$m ($\Delta kL = 20.02623$).

Acknowledgment

One of the authors, H. M. Masoudi, would like to thank King Fahd University of Petroleum and Minerals, Saudi Arabia, for their support while he is at the University of Glasgow. The authors would like to thank University of Edinburgh for the access to the Connection Machine.

References

[1] R. DeSalvo, D. J. Hagan, M. Sheikh-Bahae, G. Stegeman, and E. W. Van Stryland, "Self-focusing and self-defocusing by cascaded second-order effects in KTP," *Opt. Lett.*, vol. 17, pp. 28–30, 1992.

[2] K. Yamamoto, K. Mizuuchi, and T. Taniuchi, "Milliwatt-order blue-light generation in a periodically domain-inverted $LiTaO_3$ waveguide," *Opt. Lett.*, vol. 16, pp. 1156–1158, Aug. 1991.

[3] C. N. Ironside, J. S. Aitchison, and J. M. Arnold, "An all-optical switch employing the cascaded second-order nonlinearity effect," *IEEE J. Quantum Electron.*, vol. 29, pp. 2650–2654, 1993.

[4] D. C. Hutchings, J. S. Aitchison, and C. N. Ironside, "All-optical switching based on nondegenerate phase shifts from a cascaded second-order nonlinearity," *Opt. Lett.*, vol. 18, pp. 793–795, May 1993.

[5] D. Yevick, "A guide to electric field propagation techniques for guided-wave optics," *Opt. Quantum Electron.*, vol. 26, pp. 185–197, 1994.

[6] G. J. Krijnen, H. J. Hoekstra, and P. V. Lambeck, "BPM simulations of integrated optic structure containing second order nonlinearity," presented at the ECIO (Europ. Conf. Intg. Opt.), May 4–5, 1993.

[7] B. Hermansson and D. Yevick, "A propagation beam method analysis of nonlinear effects in optical waveguides," *Opt. Quantum Electron.*, vol. 16, pp. 525–534, 1984.

[8] P. S. Weitzman and U. Osterberg, "A modified beam propagation method to model second harmonic generation in optical fibers," *IEEE J. Quantum Electron.*, vol. 29, pp. 1437–1443, 1993.

[9] H. M. Masoudi and J. M. Arnold, "Parallel beam propagation methods," *IEEE Photon. Technol. Lett.*, vol. 6, pp. 848–850, July 1994.

[10] ——, "Parallel three-dimensional finite-difference beam propagation methods," *Int. J. Num. Mod.*, vol. 8, pp. 95–107, Mar.–Apr. 1995.

[11] Y. Chung and N. Dagli, "Analysis of z-invariant and z-variant semiconductor rib waveguides by explicit finite difference beam propagation method with nonuniform mesh configuration," *IEEE J. Quantum Electron.*, vol. 27, pp. 2296–2305, 1991.

[12] H. M. Masoudi and J. M. Arnold, "Parallel beam propagation method for the analysis of second harmonic generation," *IEEE Photon. Technol. Lett.*, vol. 7, pp. 400–402, Apr. 1995.

[13] H. M. Masoudi, "Parallel numerical methods for analysing optical devices with BPM," PhD. thesis, Faculty of Engineering, Univ. of Glasgow, 1995.

[14] M. M. Fejer, G. A. Magel, D. H. Jundt, and R. L. Byer, "Quasi-phase matched second harmonic generation: tuning and tolerances," *IEEE J. Quantum Electron.*, vol. 28, pp. 2631–2654, 1992.
[15] K. C. Rustagi, S. C. Mehendale, and S. Meenakshi, "Optical frequency conversion in quasi-phase-matched stacks of nonlinear crystals," *IEEE J. Quantum Electron.*, vol. QE-18, pp. 1029–1041, June 1982.
[16] W. H. Press, S. A. Teukolsky, W. T. Vetterling, and B. P. Flannery, *The Art of Scientific Computing: Numerical Recipes in FORTRAN.* Cambridge: Cambridge Univ. Press, 1992.
[17] M. D. Feit and J. A. Fleck, "Analysis of rib waveguides and couplers by propagation beam method," *J. Opt. Soc. Am. A.*, vol. 7, pp. 73–79, 1990.
[18] ——, "Computation of mode eigenfunctions in graded index optical fibers," *Appl. Opt.*, vol. 19, pp. 2240–2246, 1980.
[19] C. M. Kelaidis, D. C. Hutchings, and J. M. Arnold, "Asymmetric two-step GaAlAs quantum well for cascaded second-order processes," *IEEE J. Quantum Electron.*, vol. 30, pp. 2998–3005, Dec. 1994.

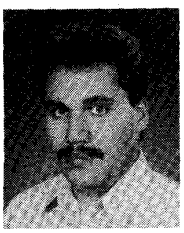

Husain M. Masoudi was born in Madinah, Saudi Arabia, in 1963. He received the B.S. and M.S. degrees from the Electrical Engineering Department of King Fahd University of Petroleum and Minerals, Dhahran, Saudi Arabia, in 1986 and 1989, respectively, and the Ph.D. degree in the field of opto-electronics from the Electronics and Electrical Engineering Department, University of Glasgow, UK, in 1995.

From 1986 to 1989, he taught undergraduate courses of electromagnetic theory, electronics and circuit analysis in the same department as a graduate assistant and a lecturer, respectively. In 1985, as part of the fulfillment of the B.S. degree, he spent seven months training on electrical power system at Chyioda Chemical Engineering & Construction Co., Yokohama, Japan. In 1990, he completed a ten-week multidisciplinary course of study and research in space subjects at the International Space University (ISU), hosted by the Institute for Space and Terrestrial Science, York University, Toronto, Canada. During his M.S. course, he worked on anomalous radio wave propagation in the atmosphere. His current interest is modeling linear and nonlinear optical devices using parallel-processing computers.

John M. Arnold was born in Sheffield, England, on August 25, 1947. He received the B.Eng (Hon.) and Ph.D. degrees in electrical engineering from the University of Sheffield in 1967 and 1974, respectively.

His Ph.D. dissertation was on the numerical modeling of thin wire antenna using the methods of moments. From 1973 to 1974, he was employed at a teacher of mathematics in the London Borough of Brent. In 1974, he was appointed as a research assistant in the Department of Electrical and Electronic Engineering, Queen Mary College, University of London, where he worked on theoretical problems in optical fiber propagation and radar scattering. In 1978, he was appointed as a lecturer in the Department of Electronic and Electrical Engineering, University of Glasgow, receiving promotions to senior lecturer in 1986, reader in 1991, and professor in 1994. His research interests center on mathematical problems in wave propagation in any medium, but particularly those involving electromagnetic and acoustic guided waves and diffraction. Nonlinear optical propagation in solid-state media is a current interest, in addition to quantum-mechanical band structure theory.